2019•2020

Faculteit Industriële ingenieurswetenschappen

master in de industriële wetenschappen: bouwkunde

Masterthesis

Shear reinforcement of longitudinal cracked glued laminated timber beams using carbon fibre reinforced polymers

PROMOTOR :

Prof. dr. ir. Jose GOUVEIA HENRIQUES

PROMOTOR :

Prof. dr. Emmanuel FERRIER

Steven Liberloo

Scriptie ingediend tot het behalen van de graad van master in de industriële wetenschappen: bouwkunde

Gezamenlijke opleiding UHasselt en KU Leuven

2019•2020

Faculteit Industriële ingenieurswetenschappen

master in de industriële wetenschappen: bouwkunde

Masterthesis

Shear reinforcement of longitudinal cracked glued laminated timber beams using carbon fibre reinforced polymers

PROMOTOR :

Prof. dr. ir. Jose GOUVEIA HENRIQUES

PROMOTOR :

Prof. dr. Emmanuel FERRIER

Steven Liberloo

Scriptie ingediend tot het behalen van de graad van master in de industriële wetenschappen: bouwkunde

UHASSELT KU LEUVEN

This master's thesis was written during the COVID-19 crisis in 2020. This worldwide health crisis has possibly impacted this assignment, investigative acts and research results.

Deze masterproef werd geschreven tijdens de COVID-19 crisis in 2020. Deze wereldwijde gezondheidscrisis heeft mogelijk een impact gehad op de opdracht, de onderzoekshandelingen en de onderzoeksresultaten.

PREFACE

This master's thesis was written during a foreign exchange programme in Lyon, France at the Université Claude Bernard Lyon 1. During my exchange, the faculty of Civil Engineering at the Institut Universitaire de Technologie (IUT) welcomed me and allowed me to research this master's thesis at its Laboratoire des Matérieaux Composites pour la Construction. Due to the COVID-19 pandemic of 2020, this exchange was cut short and I was forced to return home after only 1,5 months. Despite the difficult situation, this master's thesis was able to be completed and I want to thank both the receiving and sending institutions. This collaboration between both universities allowed me to gain unique insight that I would not have been able to otherwise.

I would like to give special thanks to professor Emmanuel Ferrier, for sharing his knowledge on composite materials and supporting this research, associate professor Cecile Grazide, for additional support during this master's thesis, and professor Jose Alexandre Gouveia Henriques, for following up on my progress and all the feedback he provided. I also want to thank the Erasmus+ programme which allowed me to do this foreign exchange and gain both personal and academic experience. Finally, I want to personally thank my mother and 2 sisters, who supported me during the whole process.

Table of contents

PREFACE 1
LIST OF TABLES 5
LIST OF FIGURES 7
ABSTRACT 9
ABSTRACT IN DUTCH 11
1. LITERATURE REVIEW 13
1.1 Introduction 13
1.2 Necessity of reinforcement of glued laminated timber structures 15
1.3 Traditional reinforcement methods and materials 16
1.4 Reinforcement using fibre reinforced polymers 18
1.5 Design considerations for reinforcement of timber 20
1.6 Possible reinforcements with FRPs 21
1.7 Failure of reinforced structures 22
1.8 Conclusion 23
2. METHOD AND MATERIALS 25
2.1 Materials used for testing 25
2.2 Debonding strength testing 26
2.3 Full scale beam testing 29
3. SINGLE LAP SHEAR TESTING 31
3.1 Results 31
3.2 Comparison with existing research 38
4. FULL SCALE BEAM TESTING 41
4.1 Results 41
4.2 Comparison with existing research 45
5. CONCLUSION 47
6. BIBLIOGRAPHY 49

LIST OF TABLES

Table 1 Characteristic strength and stiffness properties in N/mm² and density in kg/m³ [4]..... 25
Table 2 Properties of CFRP used according to [28]..... 25
Table 3 Overview of tested configurations..... 27
Table 4 Summary of all maximum loads achieved..... 34

LIST OF FIGURES

Figure 1 Comparison of strength between solid timber (C30) and glued laminated timber (GL30C). The f axis denotes the strength and the n axis is the number of samples tested. [3] 13
Figure 2: Composition of a combined cross section [4] 13
Figure 3 An example of a timber beam reinforced with basalt FRP [6] 14
Figure 4 Examples of damage in timber structures: (a) and (b) show rotting wood at the beam ends and at the joists in the timber roof truss; (c) shows a deformed timber tie in a roof structure due to overloading [9]. 15
Figure 5 Repair of timber by replacing damaged timber [10] 16
Figure 6 Reinforcement of the top of a beam using LVL (left) and steel (right) [8] 16
Figure 7 Linear elastic and elastic plastic model of a glulam beam reinforced with a steel plate in the tensile zone [11] 17
Figure 8 Strengthening of timber using steel by conversion into truss girder (left) and increasing cross section (right) [9] 17
Figure 9 Application of FRP reinforcement on-site from a roll of unhardened fabric [13] 18
Figure 10 Stress-strain curve for steel and multiple FRPs [17] 19
Figure 11 Diagram of softwood structure [22] 20
Figure 12 Application of flexible CFRP sheet to bottom of a beam (left) and the resulting reinforced beam (right) [23] 21
Figure 13 Diagram of side bonded (a), U-jacketed (b) and wrapped (c) reinforcement [25] 21
Figure 14 Strengthening of a girder using FRP rods in a near surface mounted profile and shear spiking [26] 22
Figure 15 Examples of main failure mode observed by [27] during testing 22
Figure 16 Placement of LVDTs during single lap shear tests 28
Figure 17 Placement of strain gauges during single lap shear tests 28
Figure 18 Overview of test pieces for single lap shear tests. 28
Figure 19 Overview of the reinforced beam for 3-point bending test 29
Figure 20 Detail of placement of reinforcement and strain gauges for 3-point bending test 30
Figure 21 Testing configuration for 3-point bending tests 30
Figure 22 Force-displacement graphs for all single lap shear tests 31
Figure 23 Displacement over time measured by both LVDTs 32
Figure 24 Bolt holes for L200_45 test pieces 33
Figure 25 Box plot summary of maximum load 34
Figure 26 Strain gauge measurements during loading 35
Figure 27 Strain in every sensor at different loads 36
Figure 28 L200_0_c fails in the reinforcement due to unexpected torsion during testing 37
Figure 29 L200_45_d shows a typical failure mode, with a combination of failure in resin and timber surface 37
Figure 30 L200_45_b fails partly in the timber 37
Figure 31 Average bond strength between 2 strain gauges 38
Figure 32 Force-displacement curves for the reinforced and unreinforced beam 41
Figure 33 Displacement measured in the centre of the beams 42
Figure 34 Strain gauge measurements during loading of the reinforced beam 42
Figure 35 Strain in different strain gauges at different loads for full scale beams 43
Figure 36 Shear crack after failure of the unreinforced beam 44
Figure 37 Shear crack after failure of the reinforced beam 44
Figure 38 Surface of debonded reinforcement after failure 44

ABSTRACT

Due to aging or errors during calculation or execution, strength of buildings can become insufficient. Rehabilitation of buildings can restore the required strength and due to the reduction in cost, waste and destruction of historical heritage is a more desirable alternative to demolition and rebuilding. FRPs are frequently used to reinforce concrete, but due to a lack of research cannot be used for timber. This master's thesis investigates the effectiveness of CFRP shear reinforcement of glued laminated timber and compares the results with existing research to determine if existing numerical models are accurate for this combination of materials.

First, the bond strength is analysed by executing 18 single lap shear tests, since debonding has been identified as the main failure mode. Next, the knowledge gained is applied to full scale beams which are tested using 3-point bending tests. Lastly, results are compared with existing numerical models to see if they properly predict failure strength.

For bond strength, existing models do not accurately predict experimental results, either because difference in materials is not considered or not enough configurations are tested. Full scale testing shows that shear reinforcement using CFRP works well in combination with glued laminated timber. More configurations should be tested to achieve a numerical model that can be used to predict ultimate strength, no matter the timber, FRP and bond dimensions used.

ABSTRACT IN DUTCH

Veroudering of fouten tijdens ontwerp of uitvoering kan zorgen voor een ontoereikende sterkte van een gebouw. Renovatie is vaak een beter alternatief voor sloop en heropbouw door een vermindering in kost, verspilling en vernietiging van historisch erfgoed. FRP's worden reeds gebruikt om beton te versterken, maar door een gebrek aan onderzoek kan het niet gebruikt worden voor hout. Deze masterproef onderzoekt de effectiviteit van CFRP-afschuifwapening voor gelijmd gelamelleerd hout en vergelijkt de resultaten met bestaand onderzoek om te bepalen of bestaande numerieke modellen accuraat zijn voor deze combinatie van materialen.

Eerst wordt de hechtsterkte geanalyseerd door 18 afschuifproeven uit te voeren, aangezien onthechting als voornaamste faalmodus is geïdentificeerd. Vervolgens wordt de opgedane kennis toegepast op volledige balken, die getest worden met 3-punts buigingsproeven. Ten slotte worden de resultaten vergeleken met bestaande numerieke modellen om te zien of deze de faalsterkte correct voorspellen.

Voor de hechtsterkte voorspellen de bestaande modellen de experimentele resultaten onnauwkeurig, ofwel omdat er geen rekening gehouden wordt met verschillen in de materialen, ofwel omdat er onvoldoende configuraties getest werden. Testen op balken tonen aan dat CFRP-afschuifwapening goed werkt. Maar meer configuraties moeten getest worden om tot een numeriek model te komen waarmee de ultieme sterkte kan voorspelt worden, ongeacht welk hout, FRP en hechtingsoppervlakte gebruikt worden.

1. LITERATURE REVIEW

1.1 Introduction

This master's thesis will investigate how to reinforce longitudinal cracked glued laminated timber using carbon fibre reinforced polymers or CFRPs against shear. Glued laminated timber is a timber material made from multiple slats glued together to form a member. The laminations work together to create a member with more stable dimensions, improved mechanical properties and lower variance of mechanical properties over traditional timber [1]. The improved properties lead to a more efficient use of material and reduced safety factors over solid timber [2]. The production process also allows the creation of curved members or combined cross sections, where inner laminations are made from a weaker material than outer laminations. This reduces the cost of the beams while often having little impact on strength, since the middle of the cross section experiences less stress than the outer parts in many bending cases.

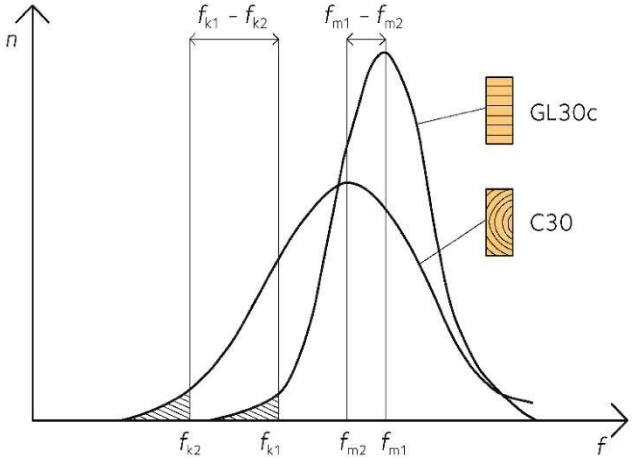

Figure 1 Comparison of strength between solid timber (C30) and glued laminated timber (GL30C). The f axis denotes the strength and the n axis is the number of samples tested. [3]

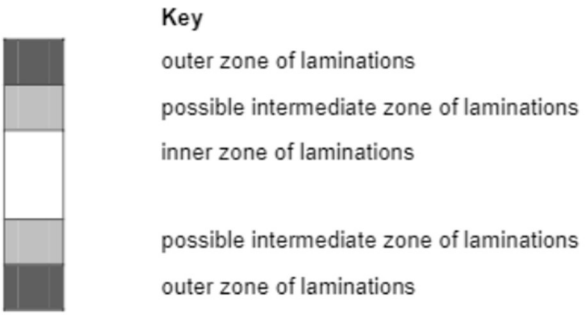

Figure 2: Composition of a combined cross section [4]

FRPs or fibre reinforced polymers consist of fibres with high tensile strength, like basalt, aramid, glass or carbon fibres, suspended in a polymer matrix, in most cases a thermoset resin. Their excellent strength-to-weight ratio makes them ideal for reinforcement of existing structures, since additional dead load is kept to a minimum. They also require a smaller cross-section for the same level of reinforcement as other reinforcement materials, like steel and timber. This allows for reinforcement of members without large changes to the dimensions of the member. FRPs also have multiple practical benefits. Firstly, reinforcement of existing members can be done with minimal disturbance of the existing structure [5]. Secondly, the fibres can be supplied to the location in flexible sheets and applied on site, making them easier to transport than steel plates for example. Finally, the existing material is mostly undisturbed, making it an excellent choice for historically significant structures.

Figure 3 An example of a timber beam reinforced with basalt FRP [6]

Before starting the research, it is important to analyse existing literature and research works to understand the current state of the art. In the first chapter, the need for reinforcement of existing glued laminated structures will be explained. Next, traditional reinforcement techniques and their shortcomings will be discussed. In the third chapter, fibre reinforced polymers as a new alternative for reinforcement of structures will be analysed. It is important to understand the specific strengths and weaknesses of each material to create an optimal reinforcement design for a structure and to avoid premature failure.

While in the previous chapters, the reinforcement materials were discussed, it is also important to have a proper understanding of the material that is being reinforced. Reinforcement of concrete structures with FRPs has been widely investigated, but timber and its properties are significantly different from concrete, which means it would be wrong to assume that FRP reinforcement will behave equally with both materials. That is why in the fourth chapter, the most important properties of timber that need to be considered are discussed. Next, past research works will be analysed to understand what is already known about reinforcement of timber with FRPs. To create an optimal reinforcement design, the limiting factors of the reinforcement need to be identified. For this reason, the sixth chapter will discuss the failure modes of a reinforced structure. Finally, the conclusion will highlight the most important aspects for this specific research topic and what the key points will be considered during testing. A list of all the resources referred to in the text can be found in the bibliography at the end.

1.2 Necessity of reinforcement of glued laminated timber structures

Glued laminated timber is a frequently used material, both in the past, present and future. However, there are plenty of factors that can render the strength of the material insufficient. Calculation mistakes, improper assumption of boundary conditions or distribution of loads can lead to improper design of the members. Timber is also susceptible to water damage, so designs that don't properly avoid surface water pooling and keep the moisture content of the timber in check, will eventually need rehabilitation. Unexpected defects in the material and errors during execution can also lead to problems with strength. Changing the purpose of a building can also change the requirements for the strength of the elements [7]. In addition, the glued laminated timber can be damaged, which can be caused by overloading of the structure, fires and thermal damage, chemical damage, biological threats like fungi, insects, bacteria and plants, water damage, sunlight and UV radiation, wear from use, ... [8].

Figure 4 Examples of damage in timber structures: (a) and (b) show rotting wood at the beam ends and at the joists in the timber roof truss; (c) shows a deformed timber tie in a roof structure due to overloading [9].

Although it is possible in certain cases to replace the components by stronger ones or to demolish the existing building and replace it with one that does meet the requirements, it is often not the best choice. Replacing buildings and building components is not a very economical approach and the creation of waste and additional consumption of material is not an environmentally friendly approach. In addition, the building can be of historical significance, where replacement of components can lead to damage of our heritage and even the components we want to replace might be of historical significance. Rehabilitation of buildings is in many cases the best solution.

1.3 Traditional reinforcement methods and materials

Traditionally, timber structures were rehabilitated using timber or steel. When rehabilitating with timber, damaged pieces of timber were cut out of the beam and replaced with new pieces of timber or additional timber material was attached to the existing beam, creating a larger cross section that is stronger. [10] describes an example of replacing timber pieces, where part of a beam was rotten due to a failure in the roofs drainage system. The decayed timber was removed and replaced with a prothesis made from laminated veneer lumber (LVL). The connection between the new and existing piece of timber was made by routing channels in the side of the beam, into which steel reinforcement was placed and bonded using a two-part epoxy adhesive. This solution can be seen in Figure 5.

Figure 5 Repair of timber by replacing damaged timber [10]

However, these methods have several drawbacks that make it an unfavourable option in many cases. Reinforcement of beams with timber requires space for the large equipment needed for the process and access to the site, both for the large timber reinforcement pieces and for the equipment. Replacing pieces of existing beams with new timber pieces can also have an unwanted effect on the aesthetics of the member. In addition, historical significance of a timber structure may prevent replacement entirely. Adding additional cross section to the member also increases the space the structure takes up, making it unusable in cases with limited room to spare.

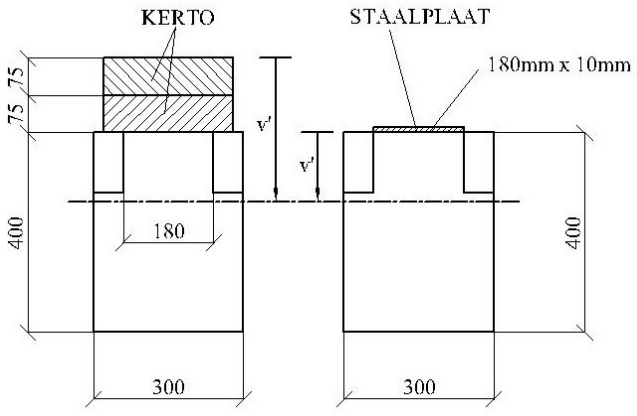

Figure 6 Reinforcement of the top of a beam using LVL (left) and steel (right) [8]

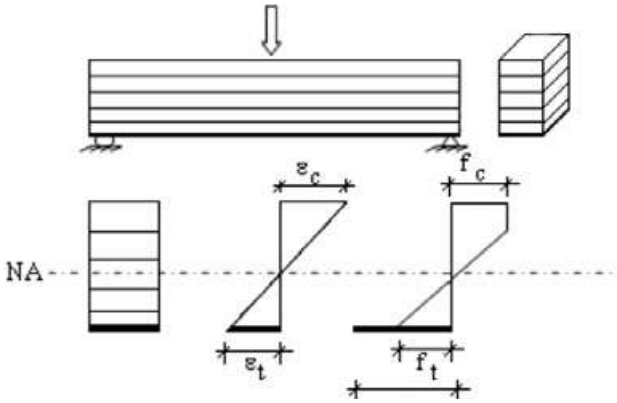

Figure 7 Linear elastic and elastic plastic model of a glulam beam reinforced with a steel plate in the tensile zone [11]

Rehabilitation using steel offers new alternatives which can solve some of these problems. When trying to increase flexural strength by creating a composite cross section, a smaller cross section is required in comparison with timber, as shown in Figure 6. This reduces some requirements for access to the site and reduces the space the reinforced structure takes up. The steel reinforcement can be attached to the existing beams using epoxy resins, mechanical connections like bolts or a combination of both. It is also possible to convert the timber beam into a truss girder to increase strength, as shown in Figure 8. However, steel has additional drawbacks: it is heavy, increasing dead loads on the structure, is susceptible to corrosive damage, increasing the required maintenance for the structure and is generally difficult to handle on site [12]. These traditional rehabilitation techniques offer solutions for some structures, but often are unfavourable or impossible.

Figure 8 Strengthening of timber using steel by conversion into truss girder (left) and increasing cross section (right) [9]

1.4 Reinforcement using fibre reinforced polymers

That is why in the late 1980s, when new fibre reinforced polymer materials became available, new methods of reinforcement were developed [7]. These use fibres with very high tensile strength, like glass, aramid, carbon and basalt fibres, bonded together to the existing component with polymers. Due to their very high tensile strength, they require a smaller cross section to achieve the required reinforcement. This makes them ideal for rehabilitation of buildings, especially ones with historical value, since the reinforced structured will not have significantly larger dimensions than the existing structure and thus does not require altering the use or the finishing materials. They are also available in flexible sheets that can be hardened on site, making them ideal for places with limited accessibility for materials. In addition, they are very resistant to corrosion when compared to steel, making them a more durable option. Finally, their high strength-to-weight ratio ensures that the additional dead load from the reinforcement is kept to a minimum [5].

Figure 9 Application of FRP reinforcement on-site from a roll of unhardened fabric [13]

While fibre reinforced polymers offer advantages over steel or timber as reinforcement, they also have specific weaknesses that need to be taken account during design and execution. FRPs are commonly bonded using organic thermoset resin, which can easily ignite, burn and produce toxic fumes. The most commonly used of these resins also lose most of their strength at a temperature between 60-100°C. Without the resin bond, the tensile stresses cannot be transferred to the carbon fibres and thus does not contribute to the strength of the composite material [14]. For this reason, FRP-composite materials in fire situations are often calculated with just the strength of the unreinforced material. In case of externally bonded reinforcement, this is a reasonable assumption, since the resin is directly exposed to fire. With timber however, the reinforcement can also be embedded in the member, giving it additional protection from fire [15]. Currently, the strength of embedded reinforcement gets ignored during fire, since there is not enough research to properly predict the contribution of the reinforcement to the total strength, but this will most likely change in the future.

FRPs also fail in a brittle manner and does not show signs of imminent failure, meaning sudden failure can have large consequences. For this reason, large safety factors are used in comparison with other materials, but this also means that most structures use more material than necessary. However, some research has been performed on so called ductile hybrid fabric, which use multiple fibres with different yield strains to create a more ductile behaviour. The research has focused on application for reinforced concrete and how the FRP reinforcement can yield at the same time as the internal steel reinforcement, increasing strength in SLS and returning the ductile behaviour of the reinforced concrete beam [16]. In the future, usage of ductile hybrid fabrics might reduce safety factors, making it an even more viable option.

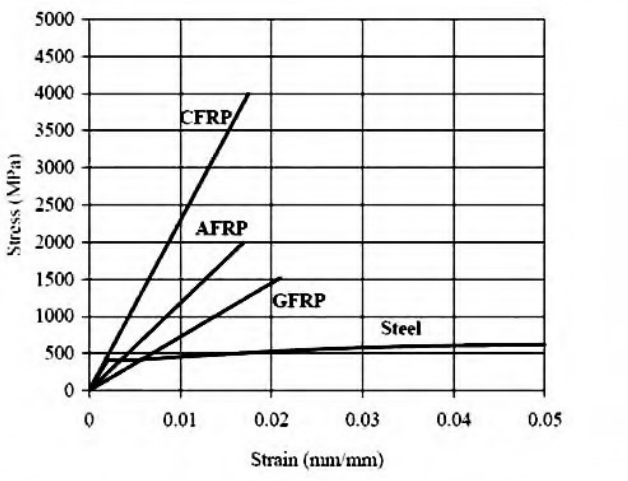

Figure 10 Stress-strain curve for steel and multiple FRPs [17]

The fibres also have high strength parallel to the fibres but are much weaker perpendicular to the fibre direction. This means that the fibres can be easily cut, which makes processing on site easy but also means that wrapping fibre reinforcement over sharp corners can accidentally cut the fibres and make the reinforcement not work as intended. For this reason, it is important to pay attention to sharp corners and round them if necessary. FRP reinforcement should also be designed to keep the fibres parallel to the load as much as possible, with secondary fibres perpendicular to the first fibres in case of loads that aren't parallel to the main fibres [18]. Additionally, current FRP solutions have high production costs, pollution emissions and energy consumption. To resolve these issues, natural fibres [19] and adhesives [20] are being investigated to offer cheaper and more sustainable alternatives.

1.5 Design considerations for reinforcement of timber

To properly design reinforcement for timber using FRPs, it is important to understand the unique properties of timber. Timber is a hygroscopic material, meaning that its volume and mass change when moisture content changes, while FRP composites absorb significantly lower amounts of moisture. In environments with continuous fluctuation of humidity, this leads to additional hygro-thermal stresses at the bonded interface and thus failure of the reinforced member at lower failure loads [21]. Reinforcement also doesn't prevent the timber members from developing cracks due to moisture cycling and should not be used for this purpose [18]. Timber is also an orthotropic material, meaning that its characteristics vary between different directions to the fibres. Timber has good compressive strength and tensile strength parallel to the fibre [6], but only has moderate shear strength, relatively low tensile and low compressive strength perpendicular the grain [18].

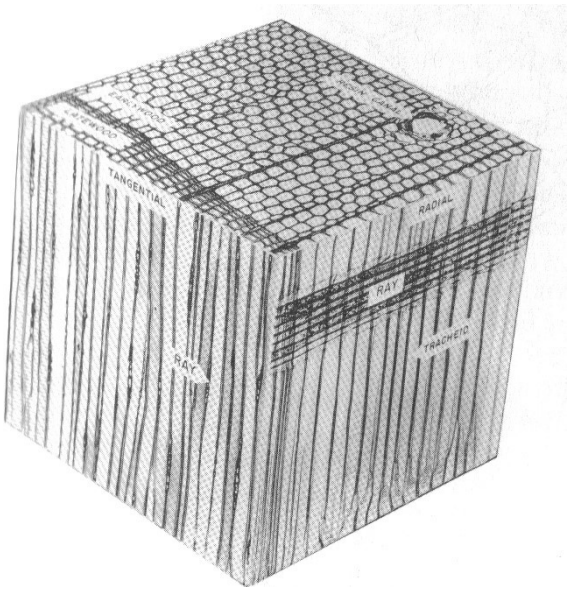

Figure 11 Diagram of softwood structure [22]

1.6 Possible reinforcements with FRPs

FRPs are available as the individual components, which get applied and cure on site, or pre-hardened plates and bars, with different mechanical behaviour observed for each solution. Unhardened fibres are flexible and can be rolled up, making them easy to transport. In cases with long members that need to be reinforced, they are also easier to handle. However, application of the resin can be messy and dangerous, requiring proper safety measures like gloves, safety glasses and a well-ventilated space. On site fabrication is also less precise than fabrication in a controlled environment, like a factory, requiring higher safety factors and thus more material.

Figure 12 Application of flexible CFRP sheet to bottom of a beam (left) and the resulting reinforced beam (right) [23]

In general, on site application of the reinforcement is mostly applied as externally bonded reinforcement, while pre-hardened plates and rods are preferred when reinforcing the beam with internal plates, near surface mounted reinforcement or shear spiking. For bending, the reinforcement should be placed as far away from the neutral axis of the beam as possible and applied lengthwise. In general, this translates to the reinforcement, hardened or not, being applied to the bottom of the cross section. For fire safety and aesthetic reasons, another piece of timber can be glued to the bottom of the reinforcement, hiding the FRP reinforcement and protecting it against fire. Shear reinforcement is more complicated, since different application methods require different designs. For externally bonded reinforcement, members can be reinforced against shear by side bonding, U-jacketing and wrapping [24].

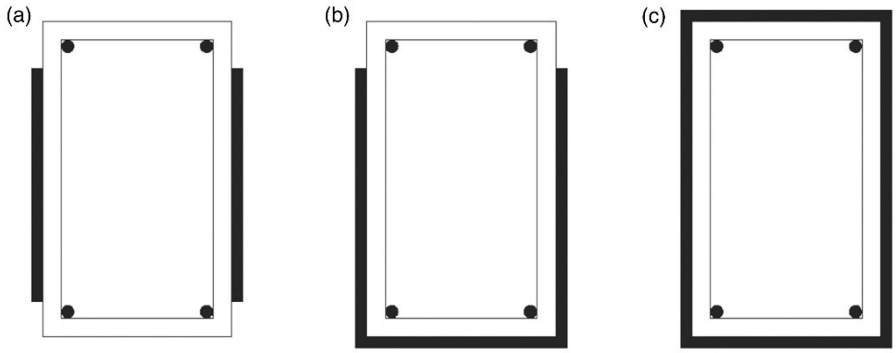

Figure 13 Diagram of side bonded (a), U-jacketed (b) and wrapped (c) reinforcement [25]

With side bonding, FRP strips get applied to the sides of the beam, while U-jacketing wraps a strip around both sides and the bottom and wrapping wraps a strip completely around the cross section.

U-jacketing and wrapping increase the bond length of the reinforcement and with it the bond strength, while using more material and requiring rounding of the corners. However, bond length has a limit [24] past which bond strength doesn't increase, making U-jacketing and wrapping unnecessary in certain cases. In practice, wrapping rarely gets applied, since in most buildings, beams support a floor and thus aren't accessible on one side. When using internal plates, reinforcement in the beam ends can increase shear capacity of a beam [15]. FRP rods can also be used as shear reinforcement with a technique called shear or "Z" spiking [26], where rods are applied through the centre of the member perpendicular to the grain.

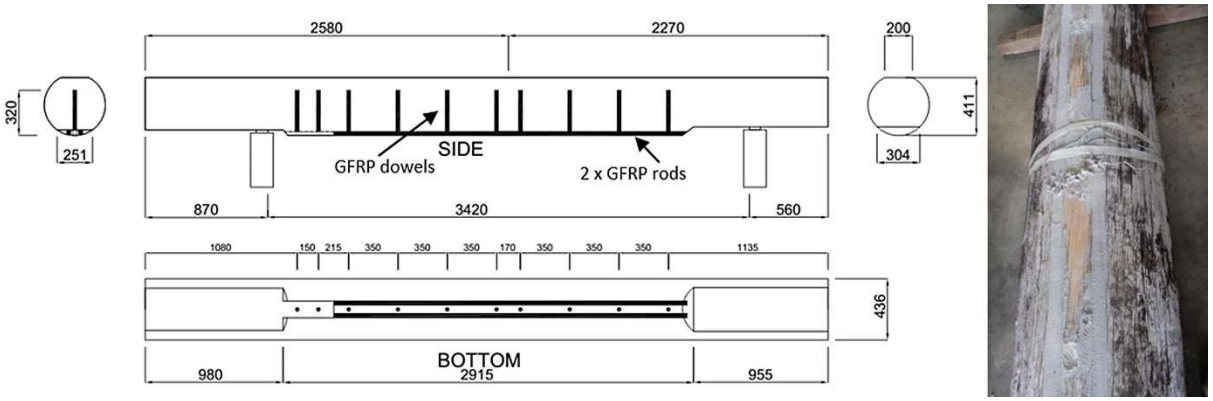

Figure 14 Strengthening of a girder using FRP rods in a near surface mounted profile and shear spiking [26]

1.7 Failure of reinforced structures

Timber beams reinforced with FRPs most often fail due to the debonding of the FRP reinforcement [27] and it is necessary to understand how and why debonding occurs to create an optimal reinforcement design. A model proposed by [27] identified bond stiffness, timber tensile strength, FRP to timber width ratio and bond length. The main failure mode identified during bond testing is substrate failure, indicating that the properties of timber determine the strength of the bond instead of the adhesive properties. However, in the most common use cases for FRP reinforcement, where a structure is being rehabilitated, the timber is part of the existing structure and cannot be changed. This makes the bond geometry the most crucial part of the design, since you always have control over it.

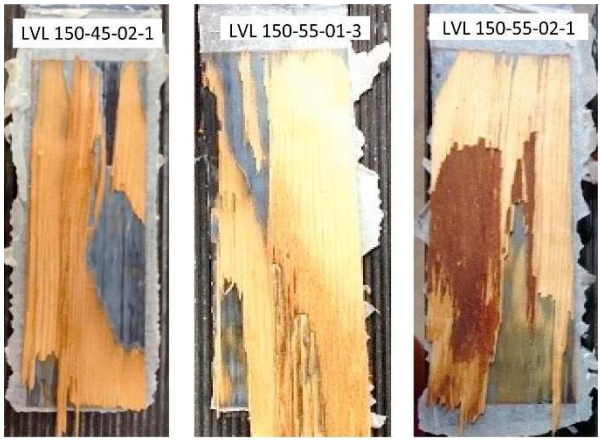

Figure 15 Examples of main failure mode observed by [27] during testing

An increase in bond width increases the strength of the bond between the two materials, reduces the slip during the softening-debonding stage and reduces the shear stress in the bond interface. A longer bond length increases the strength of the bond, but it only increases until the effective bond length is reached. The effective bond length can be determined experimentally by applying strain gauges to the reinforcement and measuring the distance between the maximum strain and zero strain. While this is a realistic method for determining effective bond length during experimental research of individual test pieces, it is not practical for reinforcement design of structures and buildings. That is why [12] suggested a formula for determining the bond strength based on the previously mentioned parameters. Currently, not enough research has been conducted to utilize this formula with certainty, especially with the wide variety of timber products on the market, but it is a solid start for our research.

1.8 Conclusion

There are a multitude of reasons why glued laminated timber structures might require reinforcement to properly carry all the loads applied to it. But traditional reinforcement techniques carry some major disadvantages (large cross sections, greatly increased dead load, difficult to install, susceptible to corrosion...), making them inefficient or even unusable options for certain projects. With the arrival of fibre reinforced polymers, new options for reinforcement arose. Multiple techniques for reinforcement using these materials exist or are being investigated, but for this master's thesis, the focus will be on externally bonded reinforcement of carbon fibre reinforced polymers.

In this literature review, several key aspects for testing CFRP shear reinforcement of glued laminated timber were identified. With debonding being identified as the main failure mode [27] of FRP reinforcement, the experiments will start by testing debonding strength and compare the results with existing models and research for timber and concrete. With timber being an orthotropic material, it would be wrong to assume bonding strength will be the same in all directions. For this reason, the experiments include test pieces with 3 different angles between the fibre direction of the timber and the reinforcement, namely 0°,45° and 90°. Bond length will also be checked with strain gauges on the reinforcement, to see if effective bond length is being achieved or not. Other aspects that influence bond strength, namely adhesive stiffness, timber strength and bond width, will be controlled during experimental testing to achieve consistent and comparable results.

Once the key aspects for the bond strength are identified, a second phase of experiments will be conducted where the reinforcement will be tested on full scale beams. This is done to see how much the strength of the beam can be improved with reinforcement and to make sure that debonding is the failure mode. The beam will be reinforced with U-jacketing, since this ensures that effective bond length is achieved and because this reinforcement technique is most likely to show other failure modes, if they occur. To make sure that the beam fails in shear, a piece of the timber beam will be cut out at one of the supports to initiate the longitudinal shear crack. Finally, all the experimental results will be compared against some of the experimental data and numerical models analysed in this literature review to see if existing methodologies can be used for reinforcement design of glued laminated timber with CFRP shear reinforcement.

2. METHOD AND MATERIALS

Before gathering experimental data, it is important to define the methodology and materials that will be used. To determine the debonding strength, experimental data will be collected using single lap shear tests. After the debonding strength is known, full scale beams will be tested using 3-point bending tests to verify that debonding is the failure mode and to compare reinforced and unreinforced beams.

2.1 Materials used for testing

The glued laminated timber used during testing was GL24h from the Margueron company in France. It consists of 11 laminations of 45mm thick, forming a final cross section of 490mm high by 210mm wide. In Table 1 the properties of GL24h timber can be found, according to EN 14080. For the CFRP the carbon TFC solution from Freyssinet was used, which consists of Foreva TFC H carbon fibre fabric and a 2 part Foreva Epx TFC adhesive. The carbon fibre fabric consists of Torayca carbon fibre rovings, which contain 12000 monofilaments of 7 to 8 microns in diameter, with glass fibres for the horizontal rovings. 70% of the rovings are in the main direction, with 30% in the secondary direction. The properties of the composite CFRP according to the manufacturer can be found in Table 2, which were translated from CSTB documentation.

Bending strength	$f_{m,g,k}$	24
Tension strength	$f_{t,0g,k}$	19,2
	$f_{t,90g,k}$	0,5
Compression strength	$f_{c,0g,k}$	24
	$f_{c,90g,k}$	2,5
Shear strength	$f_{v,g,k}$	3,5
Modulus of elasticity	$E_{0,g,mean}$	11 500
	$E_{0,g,05}$	9 600
	$E_{90,g,mean}$	300
Shear modulus	$G_{g,mean}$	650
Density	$\rho_{g,k}$	385

Table 1 Characteristic strength and stiffness properties in N/mm² and density in kg/m³ [4]

Minimum thickness	0,48 mm
Tension at rupture	1700 MPa
Modulus of elasticity	105 000 MPa
Rupture tension (for 1cm of warp)	8,15 kN
Rupture tension (for 1cm of weft)	3,50 kN

Table 2 Properties of CFRP used according to [28].

The epoxy resin came in 2 differently coloured parts and was prepared by mixing the two parts until completely homogeneous. The carbon fibres were then coated with this resin on both sides before application and the surface onto which the reinforcement was applied was also coated with resin. Next, the fibres were applied to the timber and to achieve minimal distance between the carbon fibres and the timber, any excess resin was pushed out and scraped away. Lastly, a layer of resin was applied to the top surface of the reinforcement. The resin was left to cure for at least one week before testing to ensure proper curing.

2.2 Debonding strength testing

To understand debonding behaviour and measure debonding strength, single lap shear tests will be performed. This test was chosen because it isolates the problem to only the debonding strength and allows strain gauges to be applied to the surface [5]. This setup allows strain development to be monitored throughout the applied cross-section and how it develops during loading of the beam. This allows us to confirm the effective bond length by measuring the distance between the maximal strain and nearly 0 strain. It is important to confirm the effective bond length during testing since a numerical model or formula for the specific material combination does not exist yet. The results for effective bond length will be compared to existing formulas and numerical models after testing, to see if they can be used (with or without minor adjustments) for this specific material combination.

To determine an appropriate bond length for the test pieces, both existing research and specifications were considered. The specifications [28] requires an effective bond length of 100mm for compressive strength equal to or above 25 MPa or an effective bond length of 150mm in case compressive strength is lower than 25 MPa. However, these specifications were written for application on concrete, so might not be accurate. [12] suggests an equation to determine effective bond length for FRP-to-timber joints, which might result in a more accurate effective bond length for this specific application.

$$L_e = \alpha * \beta * \ln(E_f t_f) * (f_{ut})^{0,25}$$

In this formula, L_e is the effective bond length, α is a constant with a value of 4,5π which was determined from test results, β is the FRP to timber width ratio, E_f is the modulus of elasticity for the FRP, t_f is the thickness of the FRP and f_{ut} is the ultimate tensile strength of the timber. The FRP to timber width ratio β is determined by the following formula:

$$\beta = \frac{1,25 + \frac{b_f}{b_t}}{2 * (2,5 - \frac{b_f}{b_t})}$$

In this formula, b_f is the width of the FRP laminate and b_t is the width of the timber block. The timber blocks used for testing will have a width of 490mm and CFRP reinforcement with a width of 50mm will be used. This together with the properties of the CFRP found in table 2 allows the effective bond length to be calculated as follows:

$$L_e = 4{,}5\pi * \frac{1{,}25 + \frac{50mm}{490mm}}{2 * \left(2{,}5 - \frac{50mm}{490mm}\right)} * \ln(105000\ MPa * 0{,}48mm) * (16{,}5\ MPa)^{0{,}25} = 87{,}0mm$$

Since the effective bond length is estimated between 87mm and 150mm, a bond length of 200mm was chosen for the initial testing. This allowed for 50mm of additional bond length, which is needed to be able to confirm that effective bond length is reached by measuring almost zero in the last strain gauge. However, results from the first series of 9 test pieces still showed significant strain in the last strain gauge, which prompted a second series of testing with a new configuration with a bond length of 250mm.

A summary of all the different tested configurations can be found in Table 3 Overview of tested configurations. To ensure the debonding area was not larger than desired, the rest of the area was masked off using tape with releasing agent applied to it. An additional piece of timber with the same height was used to rest the free end of the reinforcement on, to ensure that the reinforcement cured as straight as possible. To guarantee that the test machine has a good grip on the CFRP, the end of the reinforcements is strengthened with an additional 100 x 50 mm glass fibre fabric.

Name	Bond Length [mm]	# of test pieces	Angle between wood fibres and carbon fibres
L200_0	200	5	0°
L200_45	200	5	45°
L200_90	200	5	90°
L250_90	250	3	90°

Table 3 Overview of tested configurations

Strain gauges were applied to the surface of the CFRP reinforcement 50mm apart from each other. One of the strain gauges is placed outside the bonded area while the rest are placed in the bonded area, with the first of these strain gauges placed at the starting point of the bonding area. The strain gauges are placed throughout the reinforcement until the end is reached. In total, the test pieces with 200mm bond length have 5 strain gauges applied to them while the pieces with 250mm bond length have 6 strain gauges. Due to the high cost of these gauges, only a single test piece of each configuration has been tested with strain gauges. Displacement of the piece was also measured using 2 LVDTs or linear variable differential transformers. Both LVDTs are glued to the timber part of the test piece, with the first measuring the displacement between the timber and a block glued just outside the bonded zone of the CFRP. The second measures the displacement between the timber and the top of the steel bracket that holds the test piece in place. Figure 16 shows a photo of the test set up. Measurements were taken with a frequency of 2 Hz (once every 0,5s). The load was applied by pulling the piece at a rate of 1mm every 60s.

Figure 16 Placement of LVDTs during single lap shear tests

Figure 17 Placement of strain gauges during single lap shear tests

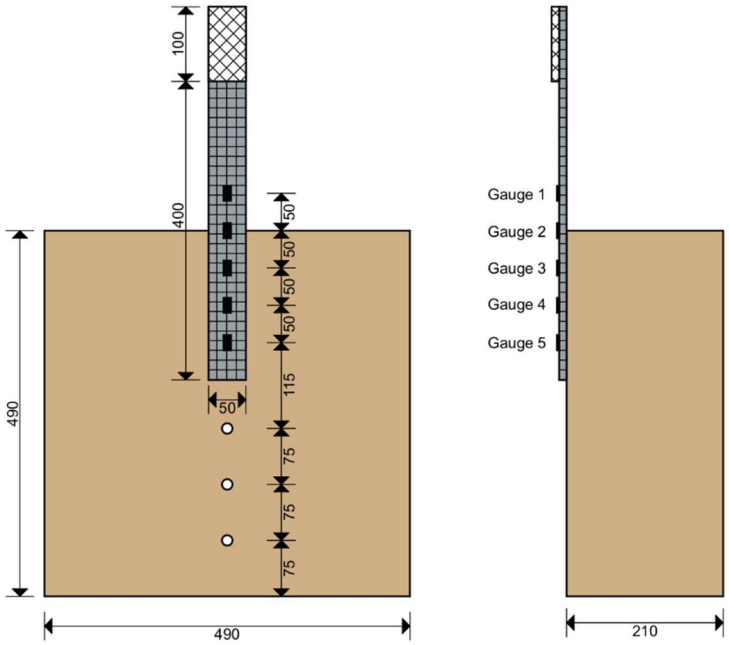

Figure 18 Overview of test pieces for single lap shear tests

2.3 Full scale beam testing

In the final stage of experimental testing, two full scale beams will be tested to confirm that debonding is the failure mode with this specific material combination and to be able to compare the strength of the reinforced beam with an unreinforced beam, existing numerical models and experimental data. Testing will be performed with a 3-point bending test in combination with a cut out at one of the beams supports to initiate a shear crack in the middle of the beam cross section. This configuration is chosen to ensure failure in shear. The initial plan for this master's thesis included 4 test pieces (2 for each configuration) but due to the Covid-19 pandemic, which closed the university where testing was performed, full scale beam testing was limited to only 2 pieces (1 for each configuration). This allows anomalies to influence the data, so results from this test are not reliable and may not represent the reality.

The dimensions of the glued laminated timber beams are 300 x 49 x 21 cm, with a cut out at one end of 38 x 24,5 x 21 cm to initiate the shear crack. One beam is left unreinforced as a control piece, with the other beam being reinforced with 3 U-jacketed CFRP strips. The strips are 75mm wide, start at the end of the cut out and are spaced 75mm apart from each other. The CFRP strips are applied to the full height and the bottom of the beam. To ensure that the fibres were not cut by sharp corners, the corners that the reinforcement wrapped over were rounded over using a router.

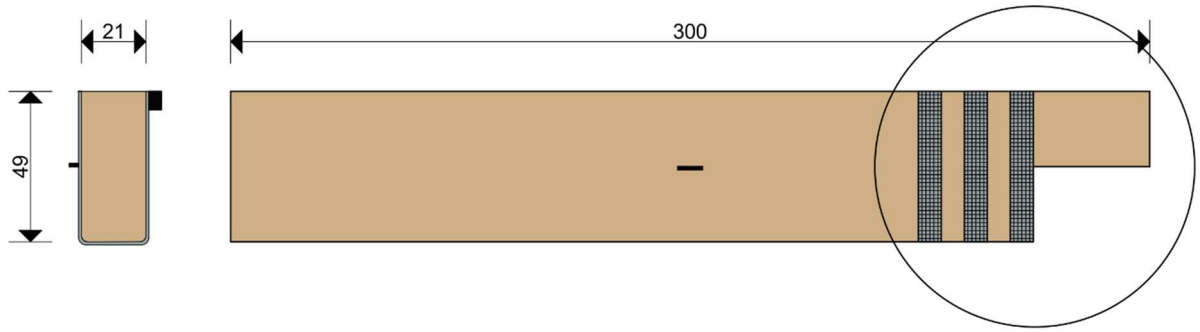

Figure 19 Overview of the reinforced beam for 3-point bending test

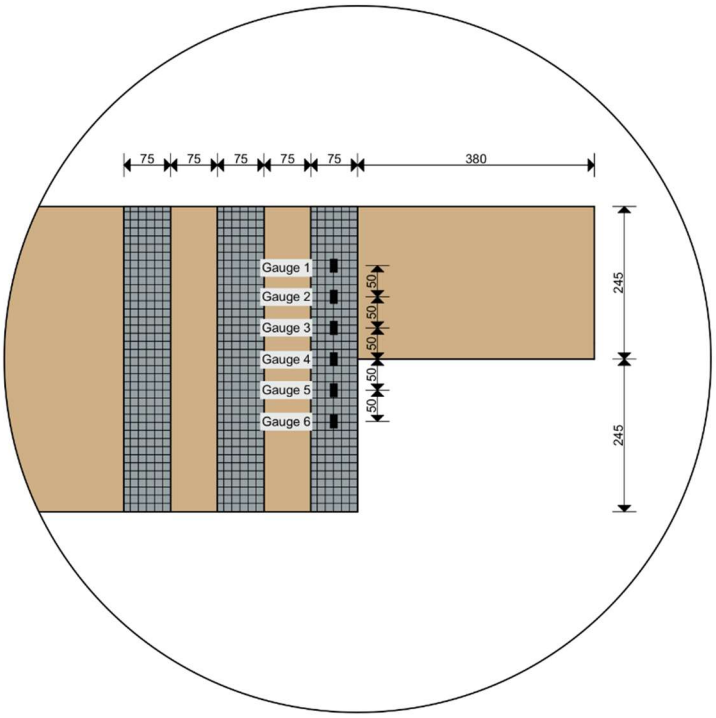

Figure 20 Detail of placement of reinforcement and strain gauges for 3-point bending test

Deflection in the middle of the beam is measured using a laser distance meter, which takes measurements from a block glued to the side of the beam at the highest point of the beam. A LVDT will also measure the deflection of the middle of the beam, but instead with the block glued to the side of the beam at half the height. In the reinforced beam, strain in one of the CFRP reinforcement will also be registered using 6 strain gauges. These strain gauges are placed 50mm apart from each other with one placed on the level where the crack will be initiated, three above the crack and two below the crack. Measurements will be taken at a frequency of 2 Hz or twice every second. The beam was loaded by pushing down at the centre of the beam at a rate of 2mm every 60s.

Figure 21 Testing configuration for 3-point bending tests

3. SINGLE LAP SHEAR TESTING

3.1 Results

Figure 22 shows the force-displacement curves for all test pieces, ordered by the different test configurations. Results are shown until the maximum force is reached, to keep the graphs easy to read. Displacement for these results were obtained by taking the displacement from the LVDT on the CFRP and subtracting any displacement measured by the LVDT on the timber. This is done to ensure only the displacement of the CFRP reinforcement is measured and not introduce additional variance due to displacement of the timber. For a majority of the tested pieces, an initial phase where force grows slowly with the displacement can be observed. This is caused by the way the tests are set up. The test piece is secured with 3 bolts but in order to easily slide in the bolts and to account for any small deviations, the holes in the timber are drilled slightly larger than the bolt diameter. When tension initially gets applied, this small margin causes a displacement of the timber with low resistance.

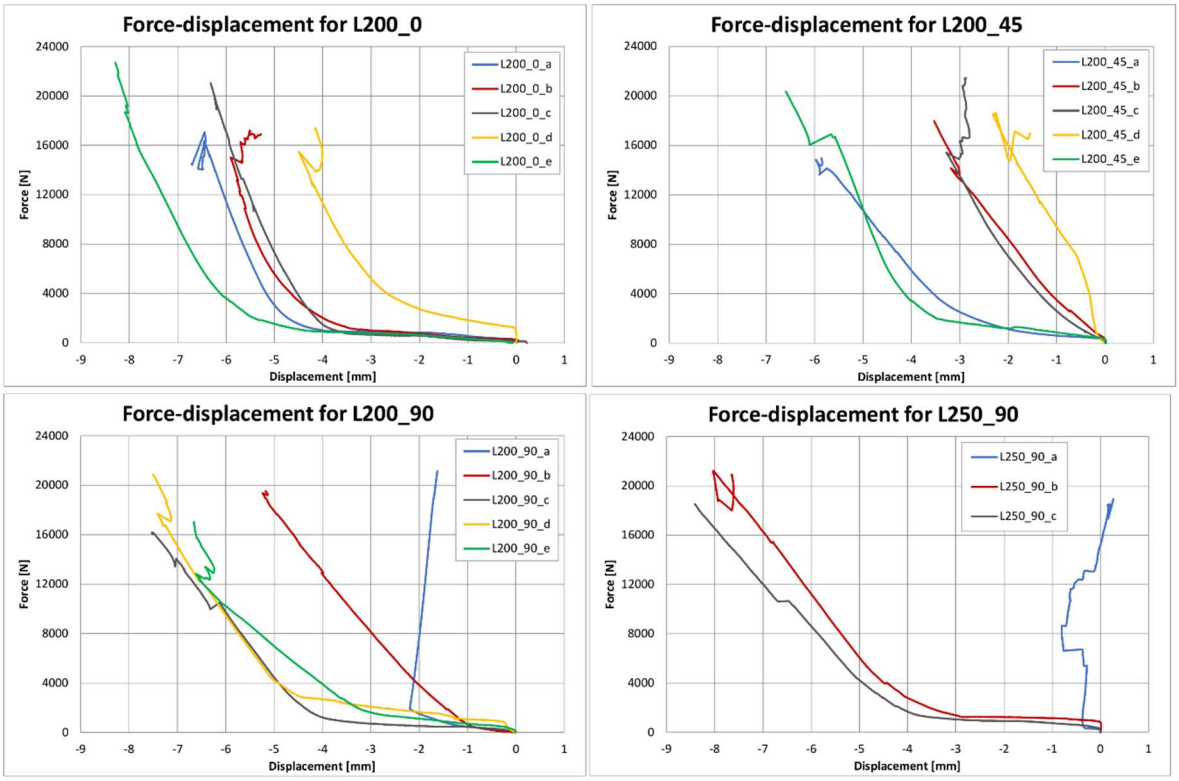

Figure 22 Force-displacement graphs for all single lap shear tests

Once the bolts provide enough resistance to the timber, the bond becomes the limiting factor and the strength of the lap joint gets tested. This lap joint loading generally shows a linear evolution over time until failure of the piece. However, a majority of the tested pieces don't show perfect linear evolution, with drops in force, displacement or both. These drops can be explained by partial failure of the bond and during testing, cracking noises could be heard at these points. In Figure 23, the displacement measured by both LVDTs is shown over time, which explains these sudden drops. For L200_45_a, a sudden drop in displacement measured by the LVDT for the timber can be observed, while the LVDT for the reinforcement doesn't experience a drop. This can be explained by partial failure of the bond, where suddenly the force applied to the timber drops and with it, the displacement. The total displacement suddenly increases at this point, while the force drops, which results in a drop in the force-displacement curve.

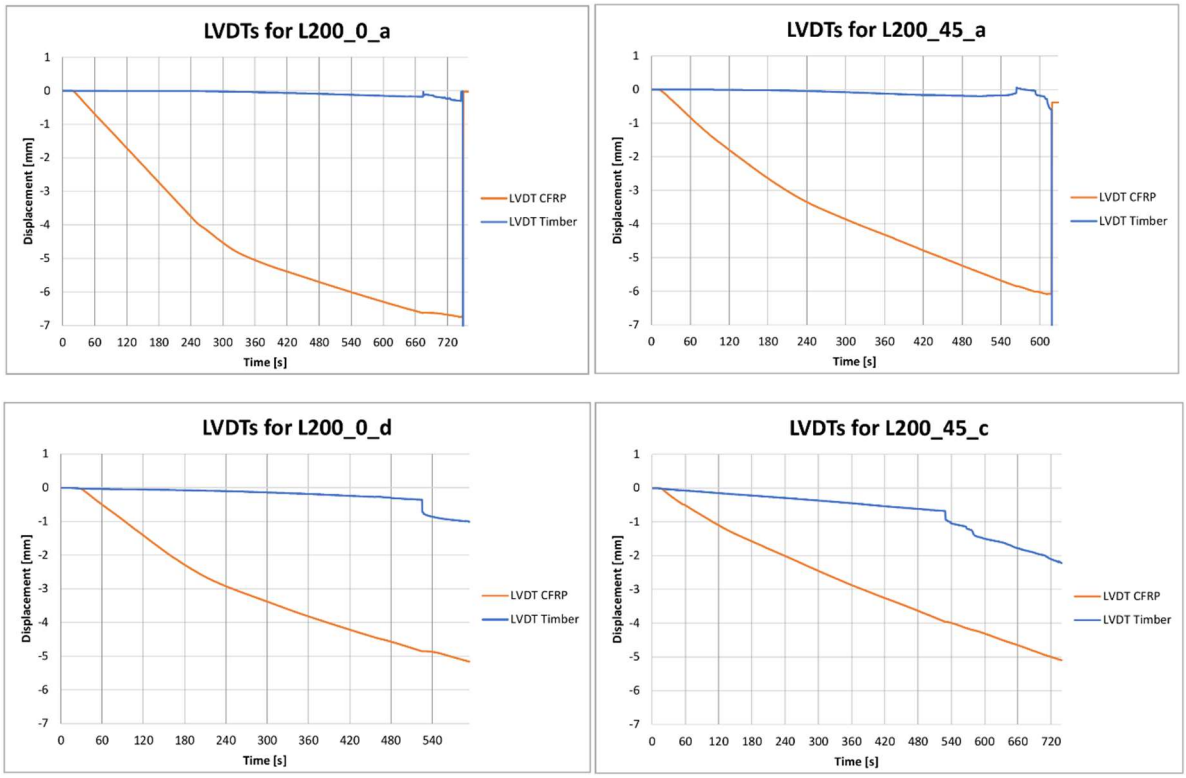

Figure 23 Displacement over time measured by both LVDTs

Meanwhile, tests like L200_0_d and L200_45_c show a different behaviour. L200_0_d shows a sudden drop in total displacement, which is caused by a sudden jump in displacement measured in the timber. At the same time, a decrease in force is also measured, which suggests that failure in the wood caused displacement of the entire piece, which reduced the force that the test setup can apply to the piece. Unfortunately, some errors in the measurements from the LVDTs occurred, which result in inaccurate force-displacement curves. The LVDTs for L200_90_a and L250_90_a produced incorrect results for the majority of the experiment, while L200_45_c only starts outputting inaccurate results after reaching about 15 000 N. Figure 23 shows why total displacement for L200_45_c stops being accurate after about 520s, with the LVDT for the timber increasing at the same pace as the LVDT for the CFRP, which results in a total displacement which stays the same.

In most cases, a sudden decrease in force can be observed before the final failure of the piece, after which the piece continues to carry the load. This can be explained by local failure of the bond caused by the timber. During these drops in load, cracking of wood fibres could also be heard. During the loading of piece L250_90_a, a small error occurred around 18 000 N. This was due to insufficient clamping pressure at the top of the CFRP reinforcement, which caused the clamp to slip instead of the bond. This resulted in an increase in displacement without an increase in load carried by the test piece. Once this behaviour was observed, the loading of the piece was momentarily paused and clamping pressure on the top of the reinforcement was increased. After the machine had enough clamping pressure to hold on to the test piece during loading, the test was continued until final failure. For the force-displacement graph in Figure 22 for this test piece, both phases are added together to show the maximum force accurately, even though displacement is inaccurate for this piece.

The L200_45 series shows differences in force-displacement development compared to the other series, which produce similar results. The initial phase, where force grows slowly with displacement due to margins with the bolt holes, is much shorter or non-existent in this series. This is likely because these pieces were attached using 4 bolts, while the other test pieces only used 3, and the pieces were tilted 45° to achieve the required angle between the CFRP and the timber. This difference in bolt holes can be seen in Figure 24.

Figure 24 Bolt holes for L200_45 test pieces

Figure 25 shows a summary of all the single lap shear tests performed, grouped by configuration. In general, there is no significant difference in bond strength between the different configurations, with less than a 5% difference between the highest and lowest average. The configuration L250_90 does show smaller spread than the other configurations, but this is most likely a result of the lower amount of test pieces for this configuration than the others and the difference is not significant enough to conclude that a bond length of 250mm decreases the variability in bond strength.

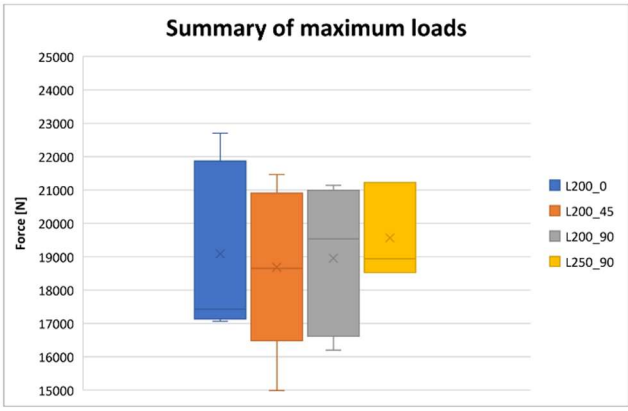

Figure 25 Box plot summary of maximum load

	L200_0	L200_45	L200_90	L250_90
a	17062,5	14987,5	21137,5	18937,5
b	17200	17975	19537,5	21225
c	21037,5	21462,5	16200	18525
d	17425	18650	20850	
e	22700	20350	17037,5	
Average	19085	18685	18952,5	19562,5

Table 4 Summary of all maximum loads achieved

For one piece of each configuration, strain was also measured during loading using strain gauges to verify that the effective bond length was achieved. Sensor 1 is the sensor highest on the test piece, placed outside the bonded zone, and the last sensor is placed lowest on the test piece, as shown in Figure 18 in the method & materials section of the paper. General development of the strain in the reinforcement is linear with force. Sensor 5 for L200_0_a produced negative strain during a large part of the test due to a problem with the sensor and should be ignored. Sensor 1 for L200_45_a also showed negative strain due to an error, but only the early stage of the test. Results for this sensor have been adjusted by removing the initial negative strain to create a more representative force-strain graph.

The strain gauges from test L200_0_a show us how the carried load can decrease slightly but not completely fail. When L200_0_a reaches 16 000 N of force, Figure 22 shows a sudden decrease in load carried by the test piece, while Figure 26 shows an increase in strain in sensor 2,3 and 4. This is most likely caused by local failure of the timber, which is confirmed by the cracking sound heard during testing, which reduces the bond surface area and thus the bond strength. However, since the piece doesn't fail at this point, the force is redistributed, increasing the strain in the carbon fibre reinforcement.

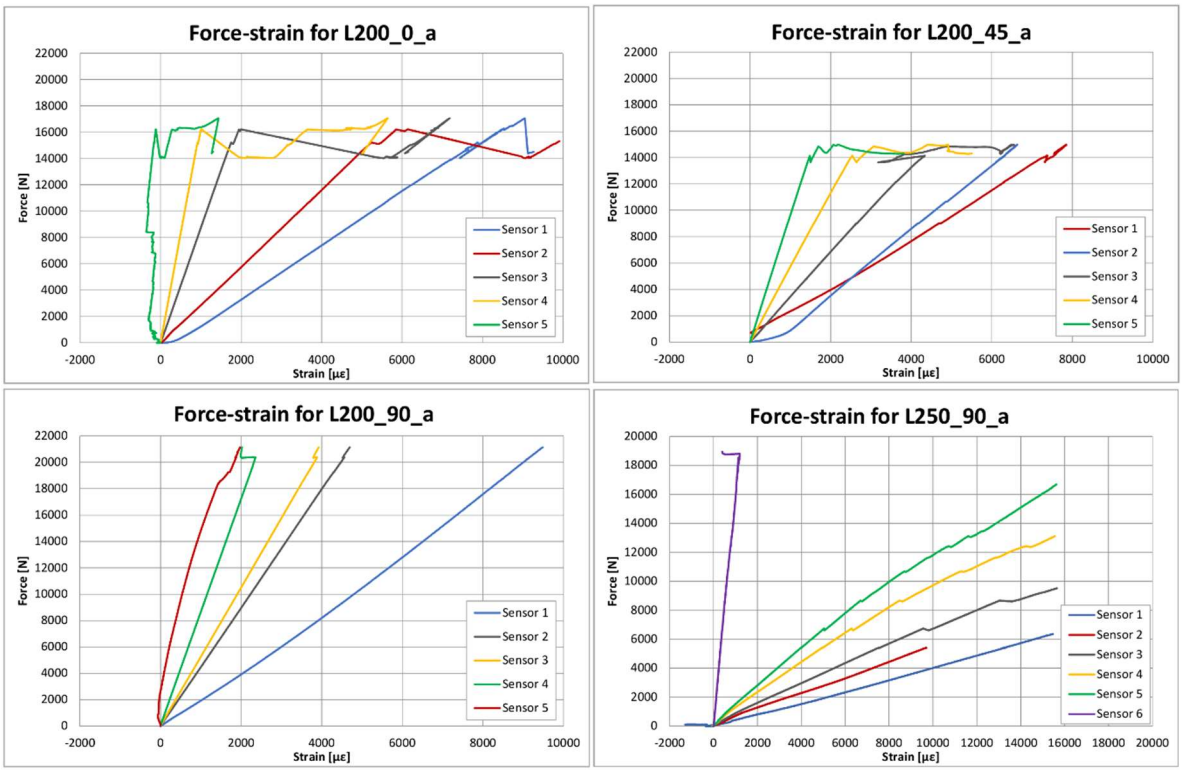

Figure 26 Strain gauge measurements during loading

Initially, the single lap shear testing was planned to be done in a single session with 9 test pieces, 3 test pieces for configurations L200_0, L200_45 and L200_90, but the results from the strain gauges were inconclusive and a second session with another 9 test pieces was performed. Strain gauge results from configurations L200_0, L200_45 and L200_90 were from the first session, while results from L250_90 are from the second session. As described in [27], when the effective bond length is achieved, strain in sensor 5 is expected to be nearly 0. As shown in Figure 27, L200_0_a shows very little strain in the sensor at 100 mm of bond length, which means effective bond length is achieved as expected. However, results for L200_45_a and L200_90_a still show a significant amount of strain at 100 mm and even at 150 mm. To ensure that higher bond strength couldn't be achieved with longer bond length, 2 additional test pieces for the existing configurations L200_0, L200_45 and L200_90 and 3 test pieces for a new configuration L250_90 were tested. This allows for the average of the existing configurations to be more accurate and the new configuration L250_90 can show if a larger bond length would result in higher bond strength and using the results from the strain gauges for L250_90_a, it can be verified if the effective bond length is reached in 200 mm of bond length or not.

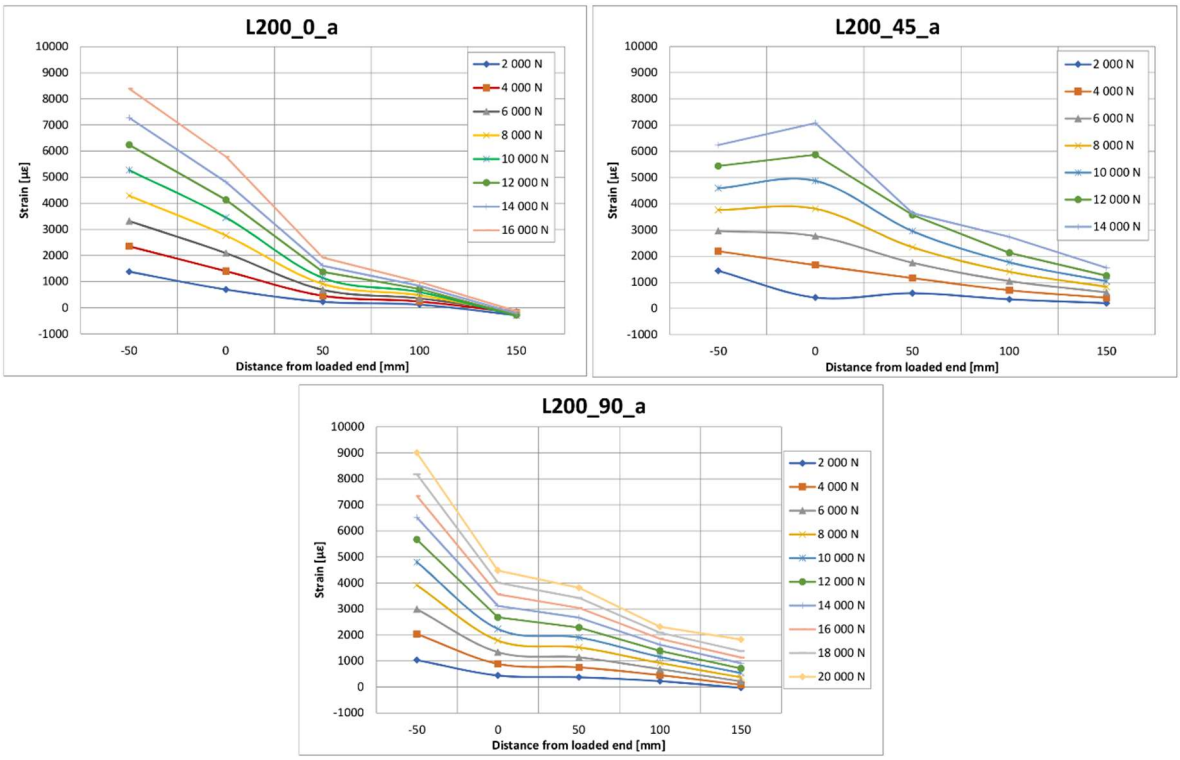

Figure 27 Strain in every sensor at different loads

Unfortunately, failure in L250_90_a was different from the others, as seen in the graph for the strain gauges in Figure 26. Strain grew much faster for this test piece and each of the strain gauges fails one by one, all at a different load. Strain gauge 2 also experienced a huge drop around 5 500 N because of an error with this sensor, so results from this sensor were cut off at this point. The strain development for L250_90_a suggests that the debonding process was gradual instead of sudden, like the other tested configurations with strain gauges applied. This means that it is impossible to verify whether effective bond length was reached using the strain gauges. However, maximum force reached by the new configuration didn't show a noticeable increase, allowing us that the effective bond length was reached within 200 mm.

During testing, failure modes were also registered and photographed. There were no significant differences between the different configurations, with no noticeable correlation between failure mode and configuration. 16 out of the 18 test pieces showed similar failure modes, with failure in the surface of the timber, in the resin or a combination of both. L200_45_c was an exception, with a small chunk of timber coming off together with the reinforcement, as shown in Figure 30. This can be explained by the high load of 20 350 N this piece resisted before failure and limited restriction of the piece of timber due to being at the point where 2 edges meet. L200_0_c also showed unique behaviour, although this was caused by the test setup instead of the materials. After around 660s, some torsion in the reinforcement was visible, which lead to partial failure in the unbonded zone of the reinforcement at around 720s and eventual full failure. This explains why its load development graph in Figure 22 looks different from the others, with a drop to 9 000 N without complete failure. The load at which this piece failed is within the range of the others, but it still failed before debonding and thus is not fully representative of the debonding strength.

Figure 29 L200_45_d shows a typical failure mode, with a combination of failure in resin and timber surface

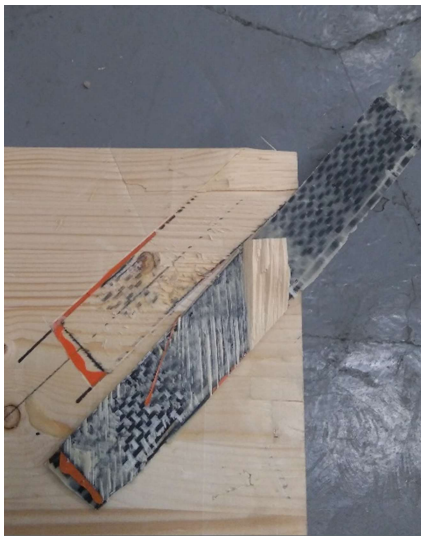

Figure 30 L200_45_b fails partly in the timber

Figure 28 L200_0_c fails in the reinforcement due to unexpected torsion during testing

3.2 Comparison with existing research

Now that the results have been analysed and summarised in the previous chapter, it is time to compare them with existing bond strength models. [27] suggested a bond strength model for LVL and hardwood based on a stepwise regression of 136 test pieces. First, the results from the strain gauges can be used with the following equation, as seen in equation (5) from [27], to plot the bond stress for different load levels at different points in the bonded length.

$$\tau_{i-j} = \frac{t_f * E_f * (\varepsilon_i - \varepsilon_j)}{\Delta l_{i-j}}$$

In this equation, τ_{i-j} is the average shear stress between two consecutive strain gauge positions, t_f and E_f are the thickness and E-modulus of the FRP reinforcement respectively, ε_i and ε_j are the strain measured at both positions and Δl_{i-j} is the distance between both strain gauges. These bond stress graphs were made only for test pieces L200_0_a, L200_45_a and L200_90_a, since they were the only test pieces with strain gauges that produced a reliable output.

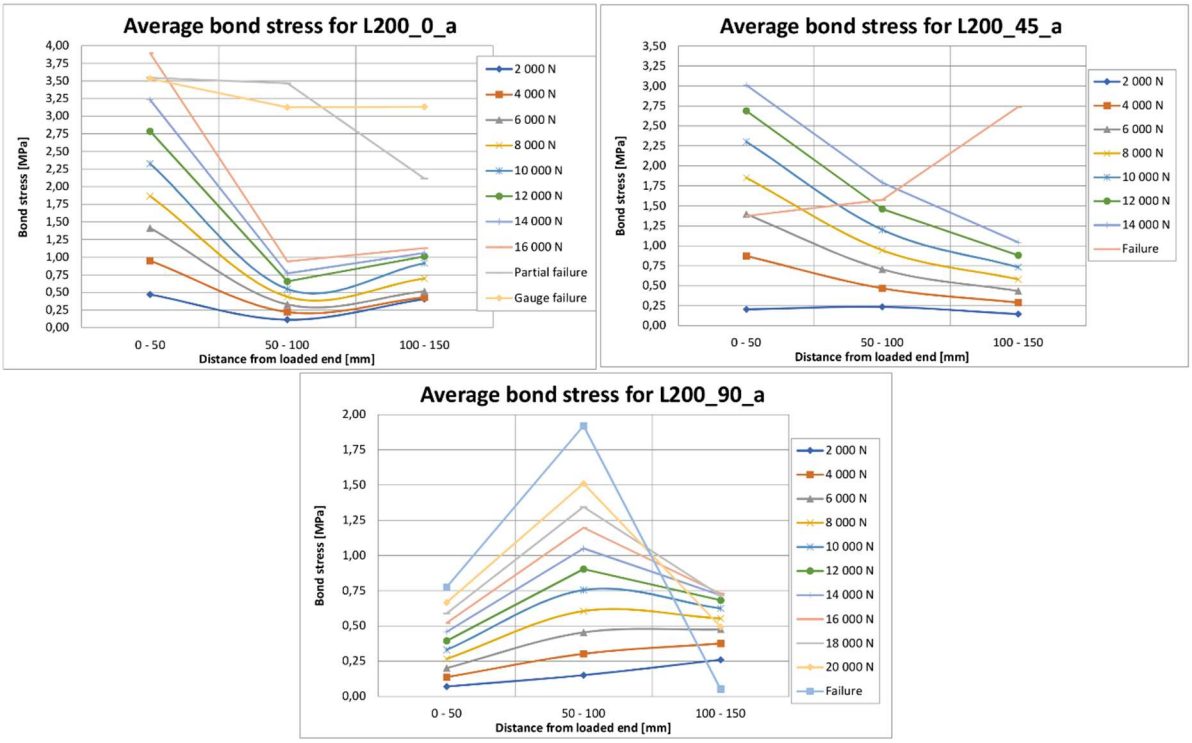

Figure 31 Average bond strength between 2 strain gauges

Although the resolution of these results is fairly low, due to the limited strain gauges used during testing, it does offer some insight into bond stresses and how these test pieces failed. Stresses are calculated every 2 000 N, just before ultimate failure for L200_45_a and L200_90_a, just after partial failure of the bond which results in a force drop for L200_0_a and just before one of the gauges fails close to final failure.

General behaviour is very similar for all 3 specimens, as shown in Figure 31: bond stress grows consistently in all the zones, until partial failure occurs in one of the zones, which can be identified by a sudden drop in bond stress. At the same time, bond stress sees an increase in one or both of the other zones. However, there are some notable differences between the different test pieces. L200_45_a shows the general behaviour the clearest: bond stress grows evenly, with the highest value in the first zone and the lowest in the last zone. This stress grows consistently until the bond start to fail between 0 and 50 mm, at which point the stresses are redistributed to the other zones. This redistribution of stresses only occurs close to failure, suggesting that the piece is unable to redistribute the stresses successfully.

Bond stress for L200_0_a is much less evenly distributed before partial failure, with the zone between 0 and 50 mm reaching the highest value out of all calculated zones. Once the bond partially fails in the first zone, bond stress drops but only by 0,348 MPa, which is much lower than in the other cases. At the same time, bond stress grows more rapidly in the other zones. The most likely explanation for these results is that the resolution is not high enough, resulting in results from the strain gauges that are not representative for the entire zone. Timber is a heterogenous material and higher strength of the material close to the strain gauge could have resulted in higher bond strength in this location. This is further confirmed by the failure force, which is not significantly higher than the other tested pieces.

Finally, bond stress for L200_90_a also gives us additional insight in the bond stress evolution. While the general evolution is as expected, the position at which highest stresses are measured and partial debonding occurs are different. Bond stress is highest in the middle rather than the start of the bonded length and partial failure doesn't occur in the zone with the highest bond stress. This could be caused by lower strength locally in the timber, in the bond or minor variance in the test setup, but the above average maximum force achieved by this piece suggest that this didn't negatively impact final bond strength.

[27] also suggested a simplified formula for calculating both the effective bond length L_e and the ultimate force that can be carried by a bond P_u. Effective bond length has already been calculated in section 2.2 of this paper and this can now be used to calculate the ultimate force. The equation for the ultimate force suggested by [27] is as follows:

$$P_u = \gamma_t \sqrt{L_e * f_{ut} * E_f t_f \left(\frac{b_f}{b_t}\right)^3}$$

In this equation, γ_t is an adjustment factor for different types of timber, with $\gamma_t = 0{,}1$ for LVL and $\gamma_t = 0{,}08$ for hardwood. L_e was calculated to be 87 mm in section 2.2 of this paper and f_{ut} is the ultimate tensile strength of the timber. E_f is once again the E-modulus for the FRP reinforcement and t_f is the thickness of the FRP, while b_f and b_t are the width of the FRP and the timber test piece respectively. Now that all necessary values are found, the equation can be filled in as follows if $\gamma_t = 0{,}1$ is used:

$$P_u = 0{,}1\sqrt{87mm * 16{,}5MPa * 105\,000MPa * 0{,}48mm * \left(\frac{50mm}{490mm}\right)^3} = 27{,}73 \text{ kN}$$

Or as follows if $\gamma_t = 0{,}08$ is used:

$$P_u = 0{,}08\sqrt{87mm * 16{,}5MPa * 105\,000MPa * 0{,}48mm * \left(\frac{50mm}{490mm}\right)^3} = 22{,}18 \text{ kN}$$

If these calculations are compared with results from Table 4, they don't match the experimental results very well. If the γ_t for LVL is used, the calculated ultimate force is too large and none of the test pieces achieve this value. If the γ_t for hardwood is used, the resulting ultimate force is closer to the experimental results but still too large compared to the averages. However, the glued laminated timber used for the experiments is made from softwood and its comparatively large laminations of 45mm might result in behaviour that is closer to softwood than LVL. Since softwood is weaker than both LVL and hardwood, a reduction in γ_t might result in a more accurate ultimate force P_u. The average ultimate load from all 18 test pieces can be used to estimate the value of γ_t for this specific series.

$$19{,}02\ kN = \gamma_t\sqrt{87mm * 16{,}5MPa * 105\,000MPa * 0{,}48mm * \left(\frac{50mm}{490mm}\right)^3}$$

$$\gamma_t = 0{,}069$$

This might be a more realistic value for γ_t for glued laminated timber made from softwood. However, the limited sample size and small number of configurations means this value should not be used outside of this paper.

$$L_e = \alpha * \beta * \ln(E_f t_f) * (f_{ut})^{0{,}25}$$

Another possibility is that effective bond length is being overestimated. In the equation for the effective bond length [27], as shown above this paragraph, has 2 factors α and β which were determined based on a linear regression analysis using the test data of the specimens from the research. Since these specimens used LVL and hardwood instead of glued laminated timber, these values might not fit the test configuration.

4. FULL SCALE BEAM TESTING

4.1 Results

To compare the load carrying capacity of the unreinforced and reinforced beams, a force-displacement graph was created, as shown in Figure 32. The displacement used for this graph was taken from the laser measurements and the graphs were cut off once maximum force was reached. Both graphs develop similarly, with an initial phase of nearly linear development of force over time until a small drop is measured, after which the force develops more slowly until the eventual failure. This drop was combined with the visible and audible development of the shear crack during testing. However, the forces at which these events occur are vastly different, with the reinforced beam needing nearly 4 times the force before the first crack starts to develop (156 688 N vs 40 813 N). Failure strength is also much higher in the reinforced beam at 187 438 N compared to the unreinforced beam, which failed at 57 250 N.

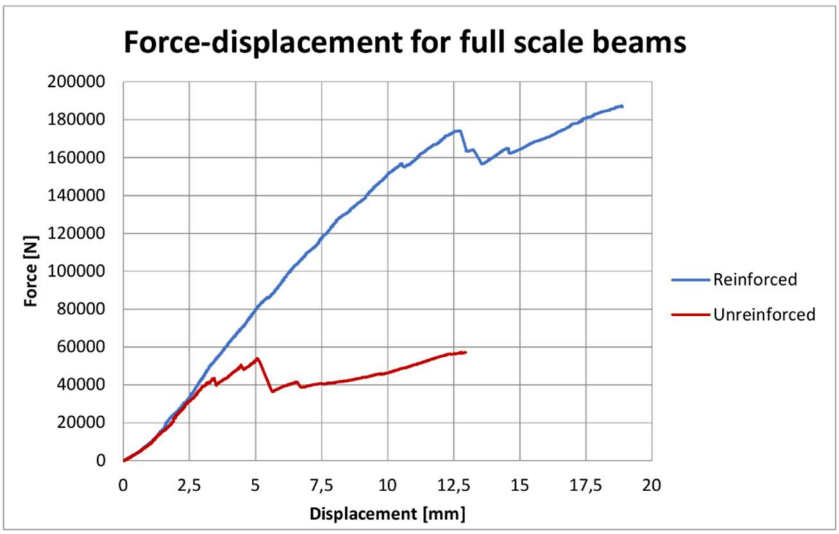

Figure 32 Force-displacement curves for the reinforced and unreinforced beam

Displacement in the centre of the beam is very similar when both beams haven't cracked, as shown in Figure 33. Once the initial crack is developed, the beams start displacing at a faster rate. The biggest difference between both beams is once again the moment at which the beam cracks and thus when the deflection increases at a higher rate. The final deflection, measured by the LVDT in the middle of the cross section, before failure is very similar, with the LVDT measuring 17,196mm in the unreinforced beam and 16,193mm in the reinforced beam. The laser measurements showed a difference, with 13,405mm and 18,88mm respectively for the unreinforced and reinforced beam respectively.

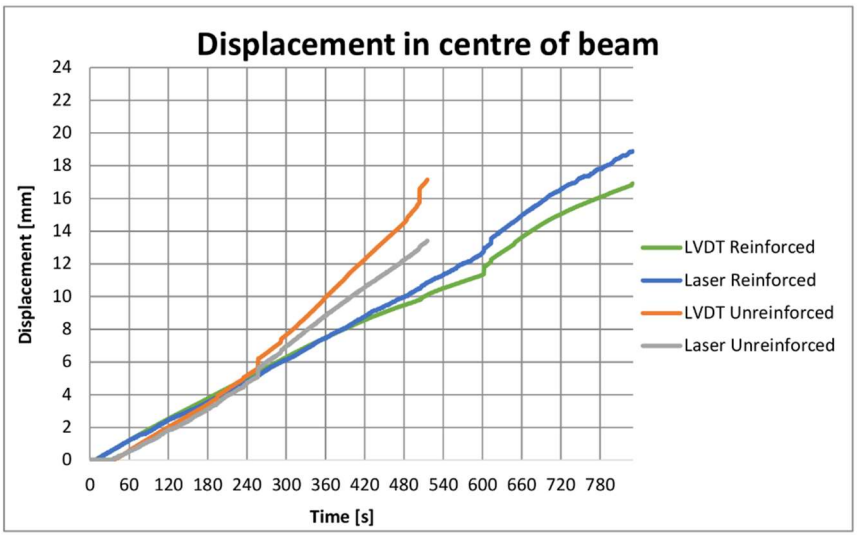

Figure 33 Displacement measured in the centre of the beams

Next, the strain in the different strain gauges is shown over time in Figure 34, where more insight is gained in how the stresses develop during loading. An initial phase where strain in the reinforcement develops slowly can be seen between 0 and 260s, after which strain develops at a higher rate. This is also the period that the unreinforced beam needed to develop its first crack. This gives reason to believe that in this initial phase, the shear force is distributed between the reinforcement and the timber, while after this phase the shear force is carried solely by the reinforcement. These claims are further substantiated by the fact that small drops in load carrying capacity show sudden increases in strain in the reinforcement.

Gauge 4 behaves differently than the others, as it reached a value of 15 859 με before failing at a force of 164 938 N, and needs further explanation. This gauge is applied to the reinforcement directly over the shear crack that is initiated. Although a small part of the sudden changes can be explained by crack development in the timber, it doesn't explain why it behaves so differently to the other gauges. However, when observing the test piece during loading, the fibres in this part of the reinforcement showed some horizontal movement. This is most likely why strain gauge 4 failed prematurely while the reinforcement did not.

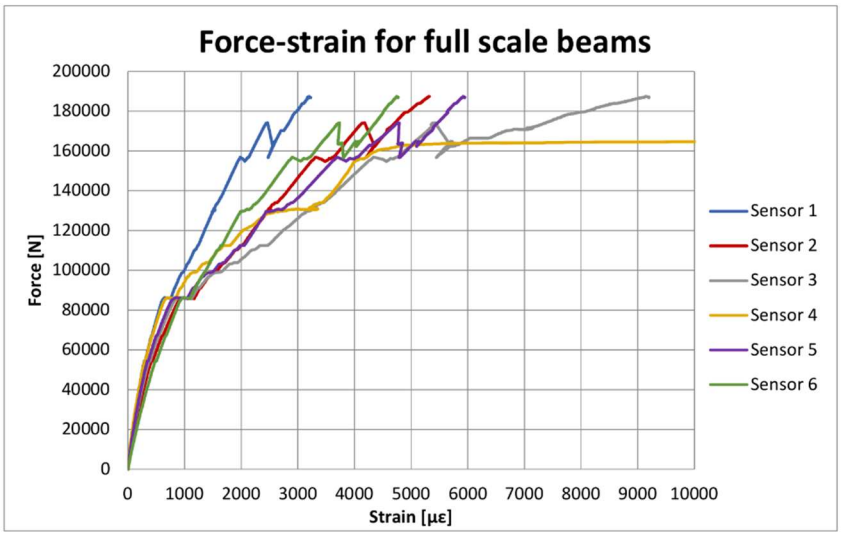

Figure 34 Strain gauge measurements during loading of the reinforced beam

Just like for the single lap shear tests, the strain is plotted for the different locations at different load levels in Figure 35. Similar strain evolution can be seen as during the single lap shear tests, suggesting that the reinforcement for the full-scale beam failed in a similar matter.

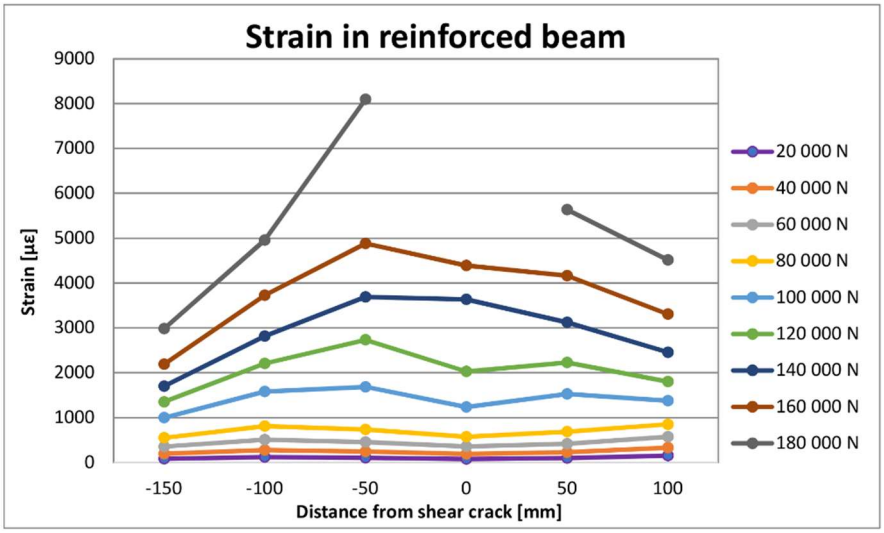

Figure 35 Strain in different strain gauges at different loads for full scale beams

Failure modes for both beams were also identified during testing. Both beams developed the shear crack as expected at the end of the cut out, although there was a significant difference in crack width. The crack was noticeably smaller for the unreinforced beam (as shown in Figure 36 and Figure 37), although this is most likely due to the much larger force being released at failure for the reinforced beam. This is further confirmed by the louder noise created by the failure of the reinforced beam. The bond surface was also inspected after failure and showed similar debonding patterns as during the single lap shear tests, confirming that the beam did indeed fail due to debonding and not another, unexpected failure mode. Figure 38 shows what the surface of the reinforcement looked like after failure.

Figure 36 Shear crack after failure of the unreinforced beam

Figure 37 Shear crack after failure of the reinforced beam

Figure 38 Surface of debonded reinforcement after failure

4.2 Comparison with existing research

In the previous chapter, the experimental data was gathered and summarized in a few graphs. Now these results can be compared against other research to determine if the combination of CFRP reinforcement on glued laminated timber beams fits existing models or if a new model needs to be developed for this specific configuration. Due to the very small sample size of only 1 for each configuration, the acquired results are very unreliable and might deviate more from the numerical model that expected.

[5] and [21] suggested the following equation to calculate the shear stresses in timber reinforced with FRP:

$$\tau_{timber,max} = \frac{V * S_{timber,max}}{b_{timber} * I_{timber}} * \frac{1 + n * \frac{h_{frp}}{h} * \alpha_{frp}}{1 + n * \frac{h}{h_{frp}} * \alpha_{frp}} * \frac{1}{1 + n * \left(\frac{h_{frp}}{h}\right)^2 * \alpha_{frp}}$$

In this formula, V is the shear force and $S_{timber,max}$, b_{timber} and I_{timber} are the static moment, width and moment of inertia of the timber. The modular ratio n can be found by dividing the modulus of elasticity for the FRP E_f by the mean modulus of elasticity E_w for the timber parallel to the grain. h_{frp} is the height of the FRP and h is the height of the timber cross-section. Finally, the area fraction α_{frp} can be calculated by dividing the area from the FRP cross-section by the timber cross section. If the equations are filled out, the results look like this:

$$n = \frac{105\,000\ MPa}{11\,600\ MPa} = 9{,}052$$

$$\alpha_{frp} = \frac{2 * 0{,}48mm * 490mm}{210mm * 490mm} = 0{,}00457$$

$$I_{timber} = \frac{210mm * 490mm^3}{12} = 2{,}059 * 10^9 mm^4$$

$$S_{timber,max} = 210mm * \frac{490mm}{2} * \frac{490mm}{4} = 6{,}303 * 10^6 mm^3$$

If these values are used together with the experimentally obtained shear forces, the shear stress can be found as follows for the reinforced specimen:

$$\tau_{timber,max} = \frac{187\,438\ N * 6{,}303 * 10^6 mm^3}{210mm * 2{,}059 * 10^9 mm^4} * 1 * \frac{1}{1 + 9{,}052 * \left(\frac{490mm}{490mm}\right)^2 * 0{,}00457}$$

$$= 2{,}624 \frac{N}{mm^2}$$

$$\tau_{frp,max} = n * \tau_{timber,max} = 9{,}052 * 2{,}624 \frac{N}{mm^2} = 23{,}750 \frac{N}{mm^2}$$

For the unreinforced specimen, the shear force can be found using the following formula:

$$\tau_{timber,max} = \frac{3}{2} * \frac{V}{A}$$

If the maximum force achieved during testing is used for this formula, the following shear stress can be found:

$$\tau_{timber,max} = \frac{3}{2} * \frac{57\,250\,N}{210\,mm * 245\,mm} = 1{,}669\,\frac{N}{mm^2}$$

In Table 1 the characteristic value can be found for the shear strength, which is 3,5 $\frac{N}{mm^2}$. While the reinforced beam has significantly higher shear stress in the timber than the unreinforced beam, both fail to reach the characteristic value. This could be because significant peeling stress occur due to the test setup, which when combined with shear stress results in lower shear strength. In the future, further experiments could be done where the peeling stresses generated by the test setup are minimized so reinforcement efficiency can be compared to the combined shear and peeling stress situation. Another option is to optimize the reinforcement for this combined load of peeling and shear stress.

5. CONCLUSION

A couple of conclusions can be taken from the investigation performed during this master's thesis. First, the angle between the fibres of the FRP reinforcement and timber does not have a significant impact on the ultimate force that a bond can carry. There is less than a 5% difference between the highest and lowest average for the different configurations. An angle of 45° does result in lower displacement during testing, but this is likely caused from the test setup and not material properties.

Second, existing numerical models cannot accurately predict the force at which the bond fails during single lap shear testing. This could be caused by factors α and β, which were obtained through linear regression analysis from [27]. This analysis only considered hardwood and LVL, not glued laminated timber or softwood, which might have produced factors that were only accurate for these materials. It is also possible that the test configurations were not different enough and only give accurate results when similar test configurations are tested. Another option is that the factor γ_t for LVL and hardwood does not represent glued laminated timber well. A more realistic value for γ_t was calculated in section 3.2 of this paper, but due to the limited number of test pieces and configurations cannot be considered as representative for every glulam-FRP connection.

Next, although the full-scale beam tests were limited to only 1 test piece for each configuration due to the COVID-19 crisis, it is clear that shear reinforcement of glued laminated timber using CFRP can greatly increase load capacity of longitudinally cracked beams. The force required for the first crack to appear was 3,84 times larger for the reinforced beam and ultimate load was increased by 3,27 times. However, due to limited testing, it is still unclear whether or not this is the most efficient way to reinforce glued laminated timber against shear. [5] states that FRP roving should be applied with an angle smaller than 90° with respect to the grain direction of the timber for a good reinforcing effect. This does mean that U-jacketing the reinforcement might not be possible anymore, but since effective bond length should be met in this configuration, this might not be an issue. The test setup used for the full-scale beam test also produced significant peeling stress, which resulted in shear stress at failure which was lower than expected.

The results from this master's thesis leave multiple opportunities for future research. While changes to the numerical model from [27] are suggested in this paper, the limited amount of test pieces and configurations makes these changes too unreliable to be used to accurately predict bond strength. Expanding the existing research with different types of timber, FRPs, bond length, bond width, timber dimensions and larger sample sizes could lead to an eventual accurate model that can be used in real world applications.

The full-scale beam testing also leaves plenty of opportunities for expanded testing in the future. Results from section 4.1 show that reinforcement of glued laminated timber beams can lead to greatly improved carrying capacity, but due to practical issues, only a single reinforcement configuration could be tested. Peeling stresses during testing were significant and lead to reduced shear stress in the timber. Due to the limited number of test pieces, the influence of these peeling stresses could not be defined and the reinforcement scheme could not be optimised for the combined stress situation. Different existing reinforcement schemes from research on concrete beams could be tested to see if similar behaviour can be observed in timber beams and possible new configurations can be created that optimize the specific interaction between FRPs and timber.

6. BIBLIOGRAPHY

[1] J. G. Henriques, Dimensioneren van hout en staal 2 [Powerpoint slides], Diepenbeek: Joint educational programme for civil engineering technology University Hasselt and KU Leuven, 2019.

[2] European committee for standardization, Eurocode 5: Design of timber structures - Part 1-1: General - Common rules and rules for buildings [NBN EN 1995-1-1:2004], Brussels: Bureau for Standardisation, 2004.

[3] A. Vahedian, R. Shrestha and K. Crews, "Experimental and analytical investigation on CFRP strengthened glulam laminated timber beams: Full-scale experiments," *Composites Part B,* vol. 164, pp. 377-389, 2019.

[4] European committee for standardization, Timber structures - Glued laminated timber and glued solid timber - Requirements [NBN EN 14080 (2003)], Brussel: Bureau for Standardisation, 2013.

[5] K.-U. Schober, A. M. Harte, R. Kliger, R. Jockwer, Q. Xu and J.-f. Chen, "FRP reinforcement of timber structures," *Construction and Building Materials,* vol. 97, pp. 106-118, 2015.

[6] E. Gomez, M. Gonzalez, K. Hosokawa and A. Cobo, "Experimental study of the flexural behavior of timber beams reinforced with different kinds of FRP and metallic fibers," *Composite Structures,* vol. 213, pp. 308-316, 2019.

[7] K. Brosens, Anchorage of externally bonded steel plates and CFRP laminates for the strengthening of concrete elements [Dissertation], Leuven: KU Leuven, 2001.

[8] S. Ignoul and K. Brosens, *Renovatie en restauratie [Powerpoint Slides],* Diepenbeek: Joint educational programme for civil engineering technology University Hasselt and KU Leuven, 2019.

[9] M. Corradi, A. I. Osofero and A. Borri, "Repair and Reinforcement of Historic Timber Structures with Stainless Steel - A Review," *Metals,* vol. 9, no. 1, p. 106, 2019.

[10] S. Franke, B. Franke and A. M. Harte, "Failure modes and reinforcement techniques for timber beams - State of the art," *Construction and Building Materials,* vol. 97, pp. 2-13, 2015.

[11] A. P. Usman and S. Sugiri, "Analysis of the Strength of Timber and Glulam Timber Beams with Steel Reinforcement," *Journal of Engineering and Technological Sciences,* vol. 47, no. 6, pp. 601-611, 2015.

[12] A. Vahedian, R. Shrestha and K. Crews, "Effective bond length and bond behaviour of FRP externally bonded to timber," *Construction and Building Materials,* vol. 151, pp. 742-754, 2017.

[13] Freyssinet, "Carbon Fibre Fabric (TFC)," [Online]. Available: http://freyssinet.bg/pageA.php?url_page3_id=18&url_lang=A. [Accessed 5 June 2020].

[14] N. Grace and M. Bebawy, "Fire protection for beams with fiber-reinforced polymer flexural strengthening systems," *ACI Structural Journal,* vol. 3, pp. 537-547, 2014.

[15] M. Morales-Conde, C. Rodriguez-Linan and P. Rubio-de Hita, "Bending and shear reinforcements for timber beams using GFRP plates," *Construction and building materials,* vol. 96, pp. 461-472, 2015.

[16] N. F. Grace, G. Abdel-Sayed and W. F. Ragheb, "Strengthening of concrete beams using innovative ductile fiber-reinforced polymer fabric," *ACI Structural Journal,* vol. 99, pp. 692-700, 2002.

[17] M. I. Khalaf, *Behaviour of RC beams strengthened with CFRP under combined actions [dissertation],* Mosul: University of Mosul, 2018.

[18] R. Steiger, E. Serrano, M. Stepinac, V. Rajcic, C. O'Neill, D. McPolin and R. Widmann, "Strengthening of timber structures with glued-in rods," *Construction and Building Materials,* vol. 97, pp. 90-105, 2015.

[19] A. Borri, M. Corradi and E. Speranzini, "Reinforcement of wood with natural fibers," *Composites Part B: Engineering,* vol. 53, pp. 1-8, 2013.

[20] H. Hoseinpour, M. R. Valluzzi, E. Garbin and M. Panizza, "Analytical investigation of timber beams strengthened with composite materials," *Construction and Building Materials,* vol. 191, pp. 1242-1251, 2018.

[21] Z. Ling, W. Liu and J. Shao, "Experimental and theoretical investigation on shear behaviour of small-scale timber beams strengthened with Fiber-Reinforced Polymer composites," *Composite Structures,* vol. 240, 2020.

[22] Arkansas Forest Resources Center, "Softwood Structure," [Online]. Available: http://www.afrc.uamont.edu/pattersond/Coursework/Undergrad/softwood_cells.htm. [Accessed 5 June 2020].

[23] S. Sheikh and Y. Ahmad, "Flexural Strengthening of Structural Timber in the 21st Century: A State of the Art Review," *Applied Mechanics and Materials,* vol. 735, pp. 128-140, 2015.

[24] J. Cheng and J. Teng, "Shear capacity of FRP-strengthened RC beams: FRP debonding," *Construction and Building Materials,* vol. 17, pp. 27-41, 2003.

[25] J. Chunyang, L. Weiwen, H. Chengyue and X. Feng, "Data analysis on fiber-reinforced polymer shear contribution of reinforced concrete beam shear strengthened with U-jacketing fiber-reinforced polymer composites," *Journal of Reinforced Plastics and Composites,* vol. 36, no. 2, pp. 98-120, 2017.

[26] J. Dewey, M. Burry, R. Tuladhar, N. Sivakugan, G. Pandey and D. Stephenson, "Strengthening and rehabilitation of deteriorated timber bridge girders," *Construction and Building Materials,* vol. 185, pp. 302-309, 2018.

[27] A. Vahedian, R. Shrestha and K. Crews, "Bond strength model for externally bonded FRP-to-timber interface," *Composite Structures,* vol. 200, pp. 328-339, 2018.

[28] Commission chargée de formuler des Avis Techniques et Documents Techniques d'Application, *Eléments des structure renforcés par collage de matériaux composites - Foreva TFC (ou TFC H),* Champs sur Marne: Secrétariat de la commission des Avis Techniques, 2017.